Study of Lateral Scaling Impact on the Frequency Performance of SiGe Heterojunction Bipolar Phototransistor

Zerihun Gedeb Tegegne, Carlos Viana, Jean-Luc Polleux, Marjorie Grzeskowiak, and Elodie Richalot

***Abstract*— The influence of the lateral scaling such as emitter width and length on the frequency behavior of SiGe bipolar transistor is experimentally studied. Electrical transistors of different emitter sizes are designed and fabricated by using a commercial bipolar transistor technology. The effect of peripheral current and collector current spreading on electrical bipolar transistor performances are analyzed in regards to the state of the art. Furthermore, the lateral scaling effect on SiGe phototransistor electrical and opto-microwave frequency behavior is studied. The impact of the lateral flow of photo-generated carriers toward the optical opening in phototransistor structure is investigated. Moreover, the 2-D carrier flow effect on the opto-microwave frequency behavior of the phototransistor is characterized through opto-microwave scanning near-field optical microscopy measurements, in the course of which the intrinsic parameters, such as transit time and junction capacitances are extracted over the surface of the phototransistor. An intrinsic optical transition frequency of 6.5 GHz is measured for 10 × 10 μm^2.**

***Index Terms*— SiGe HPT, microwave-photonics, silicon-based photodetectors, phototransistor, opto-microwave performances, OM-SNOM.**

I. Introduction

SHORT distance optical-communication systems encourage the development of optoelectronic components on a Silicon platform. In particular, ultra-low-cost silicon based optoelectronic devices are highly desirable for Radio-over-Fiber (RoF) applications within buildings and houses [1], [2]. SiGe Heterojunction bipolar Phototransistors (HPT) is one of the optoelectronic device that are recently proposed for a direct integration with a high speed SiGe technologies using standard bipolar transistors [3]–[9].

Phototransistors, which incorporate a PIN photodiode and a transistor in a single device, benefit from both photo-detection and internal amplification of the structure. Thus, it avoids the need of a Trans-impedance Amplifier (TIA) as previously studied based on InP/InGaAs HPTs [10], [11] and recently with SiGe HPTs [7], [12], [13]. SiGe HPTs were recently successfully used in a 3 Gbps signal radio-over-fiber transmission of IEEE 802.11.3c signals at 5 GHz [1].

To fabricate the HPT, the heterojunction bipolar transistor (HBT) structure is mostly enlarged, with the emitter contact limited to its original size, thus creating an optical window opening for a vertical [12], [13]. The optical window can be designed either by extending only the base and collector layers [13] or by extending the base, emitter and collector layers [12]. Thus, from the geometrical point of view, the lateral dimensions of the HBT are modified to fabricate the HPT. Therefore, the frequency behavior of the HPT is modified versus its active layers length and width.

In general the speed of semiconductor devices tends to improve as the device dimensions shrink [14]. However, according to [15], at a given minimum emitter width, the reduction of the emitter length leads to a significant reduction of speed due to the difficulties of the electron flow whereas doubling the emitter width significantly increases the speed. Our laboratory presented the first single layer SiGe HPT in 2003 [4] and we have illustrated the impact of the substrate photo-current on the speed of the HPT in [3] by using the same SiGe HPT topology. This paper is a furtherance of our previous works that explores further the frequency response limitations of the device. The main focus of this work is to envisage the lateral scaling of SiGe HPTs in order to improve their frequency behavior; and to analyses the sources of discrepancy to electrical HBT.

This paper is organized as follows. In section II describes the phototransistor structure under study, and Section III presents both vertical and lateral scaling impacts on the speed performance of the HPT. Then, Section IV focuses on the investigation of the 2-D carrier flow effects on the opto-microwave frequency behavior of the HPT via experimental results. Phototransistor scaling limitations and design rules are presented in Section V. The final section draws a conclusion on phototransistor design aspects to improve its opto-microwave frequency behavior.

II. SiGe/Si HPT Structure Under Test

The SiGe HPT is fabricated using standard SiGe2RF HBT technology from Telefunken [13]. This heterojunction bipolar transistor technology is used in wireless communication systems. The minimum emitter size on the layout of 0.8×1.4 μm^2

This work was supported by the French Government in the framework of the FUI8 Optical-Radio Infrastructure for Gigabit/s Indoor Network Project. *(Corresponding author: Zerihun Gedeb Tegegne.)*

The authors are with the Université Paris-Est, ESYCOM (EA2552), ESIEE-Paris, UPEM, Le CNAM, 93162 Noisy-le-Grand, France (e-mail: zerihungedeb.tegegne@esiee.fr; jl.polleux@esiee.fr).

Digital Object Identifier 10.1109/JQE.2018.2822179

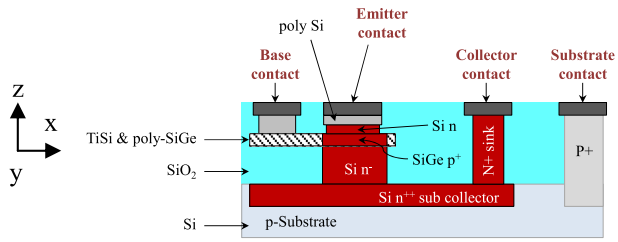

Fig. 1. Schematic cross-section of SiGe2RF technology from Telefunken.

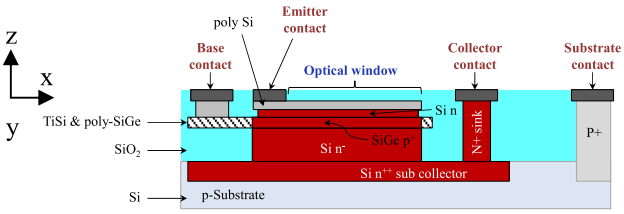

Fig. 2. Simplified schematic cross-section of an extended Emitter Base Collector HPT.

for vertical NPN HBT transistors leads to actual size after processing of $0.5 \times 1.1\ \mu m^2$ due to lateral spacers. HBT of this technology attain electrical f_T up to 80 GHz and f_{max} up to 90 GHz. This enables circuits working above 10 GHz and potentially up to 60 GHz in some configurations [16]. The general scheme of the HBT cross-section is shown in Figure 1.

The process parameters of the standard SiGe2RF HBT technology are not modified to fabricate the phototransistors. This ensures compatibility with the technological process and potential integration of circuits including opto-electronic and radio-frequency parts.

The basic HPT structure is designed by extending simultaneously the emitter, base and collector layers of the reference HBT [12]. A cross-section of the phototransistor structure is given in Figure 2. This HPT is essentially one large HBT with emitter contact restricted to the edge side of the emitter. Several phototransistors have been fabricated for this study with square optical windows of $3 \times 3\ \mu m^2$, $5 \times 5\ \mu m^2$, $10 \times 10\ \mu m^2$, $20 \times 20\ \mu m^2$, $30 \times 30\ \mu m^2$, $40 \times 40\ \mu m^2$ and $50 \times 50\ \mu m^2$. The base is made of ~40-80 nm thin abrupt SiGe layer with Ge content in the range of 20-25 % and with high p-doping in the range of $10^{19}\ cm^{-3}$ as inferred from static measurements and physical simulation comparison with earlier 50 GHz SiGe HBT generation [5], [17]. The collector is typically 300-400 nm thick and low doped. A p+ guard ring connected to the ground is surrounding the substrate region and creates a homo-junction at the interface with the p-doped silicon substrate.

In this paper, HBTs and HPTs are used in common emitter configuration. All RF measurements are performed under 50Ω load conditions on the base and collector ports through $100\mu m$ GSG RF probe.

III. Scaling Effect on Electrical Performances

In this section, we study the impact of the emitter length and width on the radio-frequency (RF) performance of HPT. For this purpose, we have fabricated seven different HBTs having

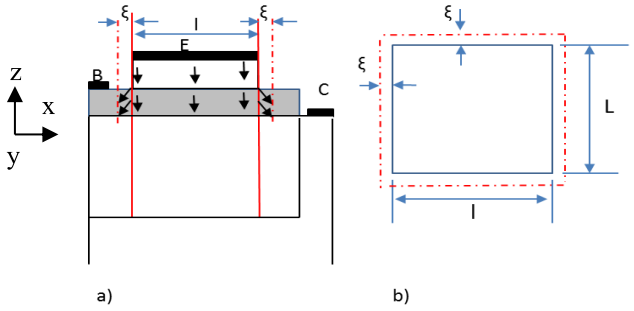

Fig. 3. Schematic a) cross-section and b) top view of the HBT of length L and width l to illustrate the influence of the peripheral region over the extension ξ.

an emitter width (along x-axis) of 0.9 μm and different emitter lengths (along y-axis). We have also fabricated seven HPTs with square optical window having different dimensions.

A. The Impact of Emitter Length on the Speed

Emitter length variation modifies the HPT/HBT speed. Therefore, looking for the optimum emitter length is crucial to design high speed HBT. The emitter-to-collector transit time delay (τ_{EC}) can effectively represent the effect of the device scaling on f_T and f_{max} as they are linked by equations (1) and (3).

$$f_T = \frac{1}{2 \cdot \pi \cdot \tau_{EC}} = \frac{1}{2 \cdot \pi \cdot \left[\frac{k \cdot T}{q \cdot I_C} \cdot C_{EC} + \tau_F\right]} \quad (1)$$

With

$$\tau_F = C_{BC}.(R_E + R_C) + \tau_b + \tau_e + \tau_{bc} \quad (2)$$

$$f_{max} = \sqrt{\frac{f_T}{8\pi C_{BC} R_B}} \quad (3)$$

where τ_F is the forward transit time, k.T/q is the thermal voltage at low injection, $C_{EC} = C_{BE} + C_{BC}$, with C_{BE} and C_{BC} are emitter-base and collector-base capacitances (which includes the depletion and parasitic capacitances), R_E and R_C are the dynamic emitter and collector resistances, τ_b, τ_e and τ_{bc} are respectively base, emitter and base-collector depletion transit time delay. These parameters are highly affected by both vertical and lateral scaling of the transistor.

The HBT can be viewed as an intrinsic transistor under the emitter and a peripheral transistor around the emitter as shown in Figure 3. According to [15], [20], and [21], the collector current I_C is the sum of the intrinsic component I_i (due to the injection of carriers within the emitter window) and external component I_e (due to lateral injection of carriers at the emitter periphery). Reducing the emitter size leads to an increase in the peripheral length-to-area ratio as shown in Figure 5. Hence the influence of the emitter periphery on the transistor behavior increases as the perimeter-to area ratio increases due to the contribution of the peripheral carriers in the total current [15], [20], [21]; in particular it can highly influence the transistor properties such as the total transit time, the junction capacitance and resistance and hence f_T.

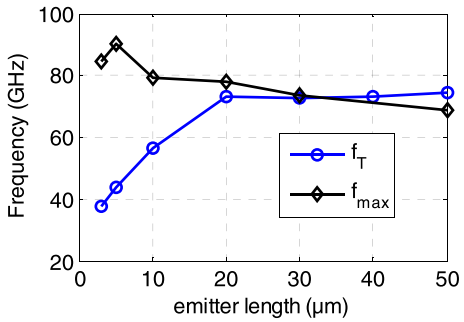

Fig. 4. f_T and f_{max} of HBTs as a function of emitter length L with a constant emitter width $l = 0.9\mu$m and for Vce=3.5 V.

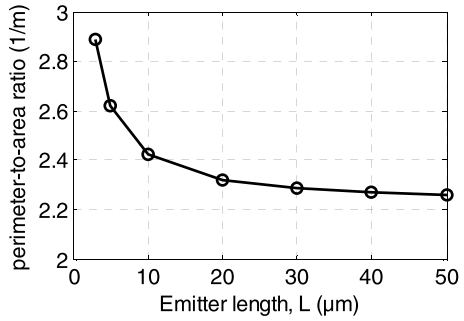

Fig. 5. The perimeter to area ratio of various size HBTs versus emitter length with a constant emitter width $l = 0.9$ μm.

Figure 4 shows the experimental result of the maximum values of f_T and f_{max} versus the emitter length. We recall the emitter width is kept constant at l=0.9 μm. The emitter-collector voltage is fixed Vce=3.5 V in this measurement. Indeed, both frequency characteristics are extracted by extrapolating respectively the device current and power gain. A significant improvement of f_T could be achieved through vertical scaling of the base, emitter and collector layers, as it leads to a significant reduction of transit time [19]. Indeed, in this study all the fabricated HBTs have the same vertical stacks, doping levels, vertical dimensions and material concentrations. Thus, only the lateral dimensions impact the f_T values.

For a given emitter width of 0.9μm, the cut-off frequency f_T increases with the emitter length from 3 μm to 20 μm before keeping constant from 20 μm to 50 μm (Figure 4). This augmentation can be attributed to the lower emitter perimeter-to-area ratio for longer emitter size (shown in Figure 5) that minimizes the relative contribution of the peripheral transit time to the total transit time. The peripheral carriers are far from the metal contacts as compared to the areal carriers and hence its transit time is larger. Thus, the peripheral component is more influent for a smaller emitter length as presented in Figure 5. In other words, the reduction of the emitter length L increases the ratio between the external and intrinsic current components, and as the path of peripheral carriers to the collector is longer, the associated transit time is higher.

The decrease of f_{max} as the emitter length increases, as shown in Figure 4, can be ascribed to the increase of the capacitance with emitter size. It is larger than f_T at low emitter length; according to equation(3), this indicates a low value of

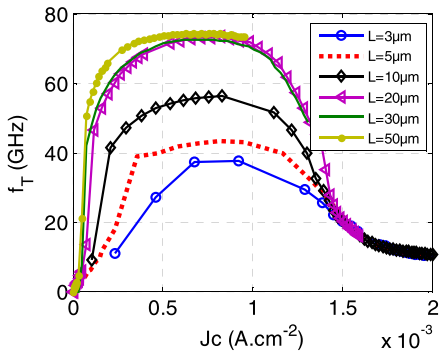

Fig. 6. f_T versus collector current density for different emitter length HBTs with a constant emitter width of 0.9 μm.

$R_B.C_{BC}$ product that is explained by a low surface capacitance. On the other hand, the $R_B.C_{BC}$ product is supposed to be constant with emitter length variation, but the experimental result shows that the variation of the device capacitance is indeed faster than the base resistance. f_{max} is smaller for emitter length equal to 3 μm than the one for 5 μm. This is due to the lower value of f_T for 3 μm long HBT compared to 5 μm HBT.

Figure 6 represents the variation of f_T as a function of the collector current density for different emitter length HBTs. At high injection level (current densities above 1.5 mA.cm^{-2}) all the curves are overlaid; this confirms that the injection level is mostly controlled by the doping levels which are the same for all HBTs. The maximal f_T values are all obtained in the same medium current density region (around 0.7 mA.cm^{-2}) and increase with the emitter length. Indeed, the level of f_T peak value is controlled by peripheral carrier contribution leading to a significant f_T reduction for small emitter length.

Three regions can be distinguished in Figure 6:

1. *Low current densities:* at a very low current density, f_T quickly increases with the collector current density as the junction capacitance reduces with the dc supply. As the transit time of the electrons injected at the periphery is larger than the internal injected electron transit time, the value of f_T at low current density is lower for smaller emitter size (smaller emitter length has more peripheral electrons than the internal electrons).
2. *Medium current densities*: this is the region before the critical current density which is defined as the onset of high injection in [15] where f_T reaches its peak. As the intrinsic conductance decreases, the capacitance charging time becomes smaller than the forward transit time. As a consequence, the device speed is mainly limited by both areal and peripheral transit times. The effect of the peripheral transit time is predominating in device whose emitter length is smaller than 20 μm as the peripheral carriers are numerous [15], [20]. In larger emitter size HBTs (L >= 20μm), the peripheral carriers are negligible and hence the speed is limited by areal transit time.
3. *High current densities:* in this region, not only the peripheral injection is responsible for the quick roll-off of f_T, but also the emitter current crowding and

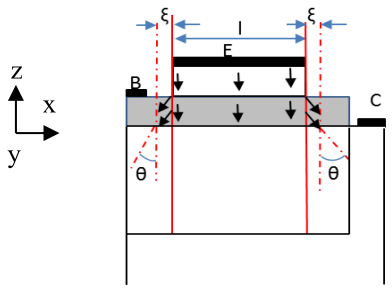

Fig. 7. The simplified cross-sectional view of the transistor that indicates the impact of the peripheral current and the collector current spreading. The θ is the angle of current spreading in the collector.

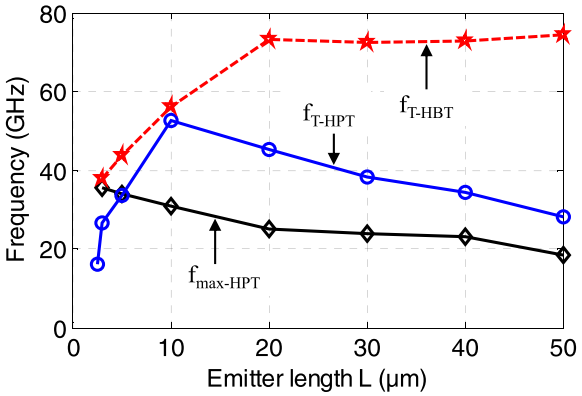

Fig. 8. f_{T-HPT}, f_{T-HBT} and $f_{max-HPT}$ as a function of emitter length L for a constant emitter width of l=0.9 μm. For HPTs, the optical window W and emitter length L as shown in Figure 9 have equal dimension whereas for HBTs W=0 μm along x-axis.

the current spreading in the collector region (shown in Figure 7) [14], [15]. At high current densities (above 1.5 mA.cm^{-2}), the reduction in f_T is observed for all transistors and similar values are obtained whatever the emitter length is.

B. Impact of Optical Window Size on HPT's Speed

An HPT is a transistor with an optical opening for light injection, as described in section II. The extended part of the phototransistor (optical window) modifies the electrical behavior of the transistor due to additional parasitic effect related to the increase in emitter width.

Figure 8 shows f_{T-HPT}, f_{T-HBT} and $f_{max-HPT}$ as a function of the emitter length L. f_{T-HPT} and f_{T-HBT} are extracted from the HPT (where the optical window W=L along x and y axes see Figure 9) and HBT (where W=0 μm along x-axis for the same L) respectively. The maximum of f_{T-HPT} appears for a width of 10 μm. In the HPT case, the increase in emitter length is connected to the increase in the optical window size W, as it is a square shape. The electron path from the emitter to the collector contact is then increased by the width W. The related R_C resistance is thus almost constant (the path is wider but also longer) and the capacitances increase. Therefore, the decrease of f_{T-HPT} as the optical window widens is due to the $R_C.C_{EC}$ term influence which become predominant in HPT structure. The smaller values for width below 10 μm are explained by

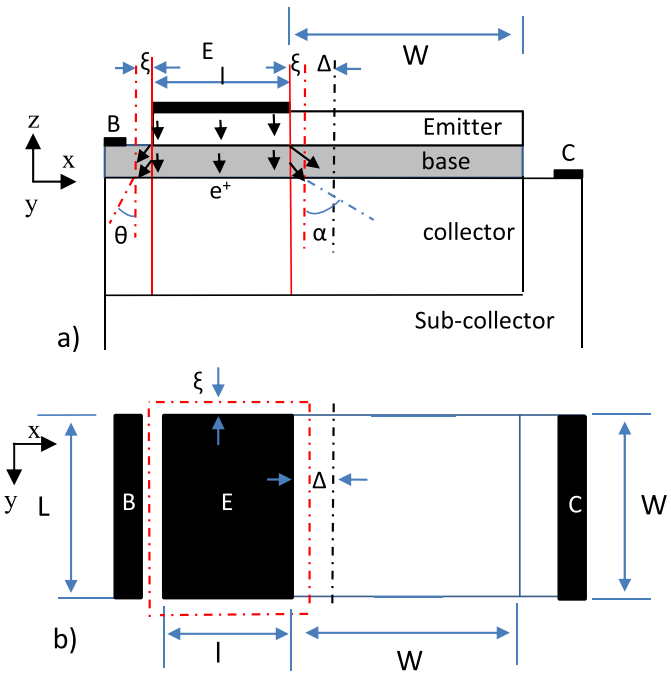

Fig. 9. The simplified a) cross-sectional and b) top view of the transistor that indicates the impact of the peripheral region ξ, the collector current spreading region θ and lateral extension into the optical window Δ.

the influence of the peripheral carriers, including lateral path region Δ and collector current spreading effect (see Figure 9), whose impact is higher with smaller window size.

On the other hand, $f_{max-HPT}$ decreases as the optical window size increases. This is due to the base resistance and base-collector junction capacitance increase with the optical window size.

In the HPT structure, we believe that the total optical window size (see Figure 9) may not act electrically as an active transistor. We believe that the area under the emitter contact may be the only active area of the transistor with however a partial spreading of the electrical active region in its vicinity into the optical window. Hence the effective active area of the transistor is modulated in size due to the dc supply bias. That means due to the dc bias the effective active region of the transistor could be extended into the optical window as shown in Figure 9 by the lateral extension region Δ. This region is actually a consequence of the inhomogeneity of the base-collector potential due to the asymmetrical design of emitter-base-collector contacts. The extension of the electrical region, Δ, is also dependent on the optical window size [13]. It increases as the size decreases.

As a result, the peripheral carrier effect mentioned for HBT structure is increased in HPT case due to this additional lateral path Δ and the increase of the collector current spreading angle α towards the optical window ($\alpha > \theta$) as shown in Figure 9. In this region, the carriers move both vertically and laterally hence the transit time to reach their respective contacts is increased. At the same time, the collector current spreading is also enhanced compared with HBT having the same length. The junction capacitances increase along with

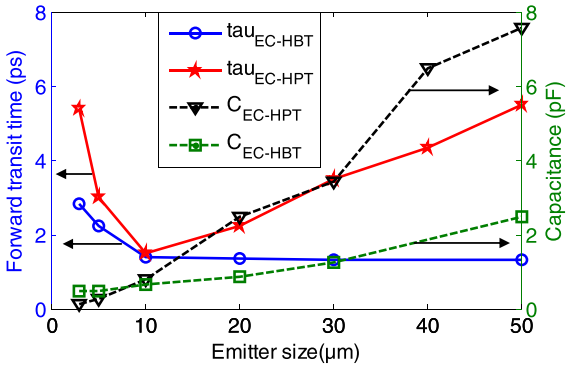

Fig. 10. The extracted electrical transit time and junction capacitances as a function of emitter length L for HBT (with l=0.9 μm) and HPT (with l=L) structures.

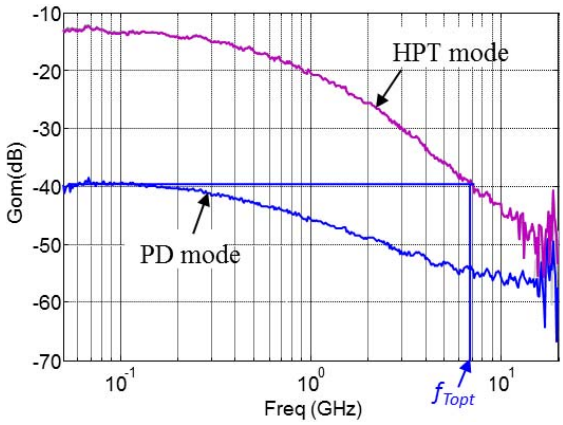

Fig. 11. Opto-microwave gain inthe photodiode (Vbe=0 V, Vce=3 V) and phototransistor (Vbe=0.857 V,Vce=3 V) modes of 10 × 10 μm^2 optical window HPT.

the extended active layers. Hence the cutoff frequency could decrease.

To demonstrate this assumption, the forward transit time and junction capacitance of the HPT and HBT are extracted experimentally. These values can be easily extracted from a plot of the emitter-collector time delay (τ_{EC}) versus $1/I_C$ according to equation (1): the junction capacitance is extracted from the slope and the forward transit time is given by y-intercept. The extracted values of the HBT and HPT as a function of the emitter size are shown in Figure 10. We recall that HBTs are fabricated by keeping the emitter width to l=0.9 μm with various emitter lengths L, whereas for HPTs the extended optical windows size W and the emitter length L are equal and take several values. From Figure 10, we draw the following observations:

1. *HBT:* The transit time (τ_{EC-HBT}) rapidly decreases for emitter length below 10 μm. Thus, it indicates that the contribution of the peripheral carrier is higher with smaller HBT. Then the forward transit time slightly decreases as the emitter length increases from 10 μm to 50 μm. The junction capacitance increases as the size keep increasing.
2. *HPT:* Similar to the HBT, the transit time (τ_{EC-HPT}) decreases versus emitter length below 10μm. However, unlike the τ_{EC-HBT}, the τ_{EC-HPT} increases further for emitter length higher than 10 μm. This is explained by the $R_C.C_{BC}$ term becomes predominant. The junction capacitance also increases with optical window size increases.
3. *Comparing HBT and HPT:* According to [15], the forward transit time should decreased versus emitter width for a given emitter length. In other words, the forward transit time in HPT should be smaller than in HBT as the emitter width of the HPT is enlarged to create the optical window for a given emitter length. However, the forward transit time in HPT is larger than in HBT. This can be explained by the fact that, in a phototransistor structure, in addition to the peripheral current and collector current spreading effects, the lateral extension Δ takes place. As a result the lateral path length for the electrons between the emitter to the sub-collector dominates over the vertical path length, which thus increases the overall transit time in HPT structure.

For the HPT structure, the extracted capacitance is supposed to have a parabolic shape with respect to the emitter length (due to the square optical window whose surface is the square of the emitter length). However, the electrical active area of the HPT is restricted to the area situated under the emitter contact (which is 0.9μm wide) and the lateral extension towards the optical window (indicated by Δ in Figure 9). Thus, the capacitance is directly related by $(0.9 + \Delta)$*L and varies linearly as shown in Figure 10.

IV. 2-D Carrier Flow Effect on the HPT Opto-Microwave Frequency Response

The opto-microwave gain (Gom) of the HPT represents the ratio of the HPT output signal power to the output power of a photodiode with a 1A/W responsivity and loaded by 50Ω [5] [13]. This is of particular use as it is equal to the square of the HPT responsivity (so the same value in dB) under a 50 Ω loading condition. It can be deduced from the S-parameter measurement [5], [13]. To characterize the opto-microwave behavior of the HPT we follow the measurement test bench set up described in [13].

Figure 11 shows the Gom versus frequency of 10×10 μm^2 optical window size HPT. The phototransistor mode (HPT mode) is obtained by setting Vbe=0.857 V and Vce = 3 V and the photodiode mode (PD mode) is obtained by setting Vbe = 0 V and Vce=3 V. The substrate contribution is removed according to [13].

Optical transition frequency (f_{Topt}) is the frequency at which the Gom of the HPT in phototransistor mode is equal to the low frequency Gom in photodiode mode as shown in Figure 11. Compared to f_T, f_{Topt} is influenced by additional terms related to the photo-detection mechanism. In addition to the pure electrical effects (such as the peripheral ξ and lateral Δ carrier effects), the opto-microwave cutoff frequency is mainly limited by the transit time of the photo-generated carriers and the increase injunction capacitances due to photo-detection mechanism. Under illumination condition the

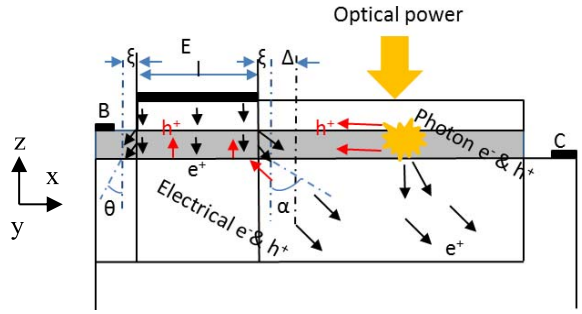

Fig. 12. The simplified cross-sectional view of the phototransistor that indicates the peripheral region ξ and its dissymmetric enlargement Δ, the collector current spreading region θ, and the photo-generated carrier flow.

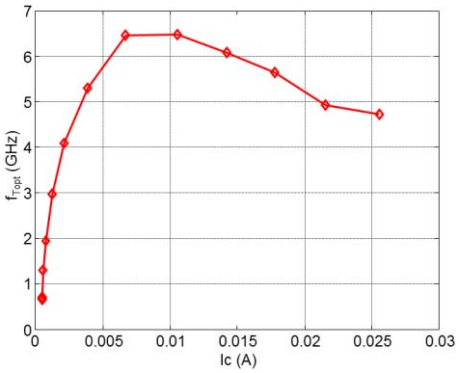

Fig. 13. The optical transition frequency f_{Topt} versus collector current when the optical beam is injected to maximize this frequency.

photo-generated electrons and holes take long time to reach to their respective contacts; and the active region extended to all region of the device as shown in Figure 12. Therefore, we propose to expand equation (1) by expressing the increase in capacitance and transit time terms of the HPT that affects the frequency response as follows:

$$f_{T\,opt} = \frac{1}{2 \cdot \pi \cdot \tau_{EC\_opt}} = \frac{1}{2 \cdot \pi \left[\frac{k \cdot T}{q \cdot I_C} \cdot \left(C_{EC} + C_{EC\_opt} \right) + \tau_F + \tau_{F\_opt} \right]} \quad (4)$$

where τ_F is the electrical forward transit time from emitter to collector, C_{EC} is the electrical junction capacitance (without light effect), τ_{F_opt} and C_{EC_opt} are the additional forward transit time and junction capacitance due to the photo-detection mechanism.

To study the opto-microwave frequency behavior, we focus on the 10×10 μm^2 optical window size HPT as it reaches the highest f_T value among other HPTs (Figure 9). Figure 13 shows the extracted optical transition frequencies f_{Topt} versus collector current (I_C). The presented optical transition frequency are measured after displacing the illuminating optical fiber above the optical window in order to maximize this frequency; thus the plotted values correspond to optimal ones in regard to the illuminating fiber position. The maximum value of f_{Topt} reaches 6.5 GHz which is very small compared to f_T value obtained with the same transistor

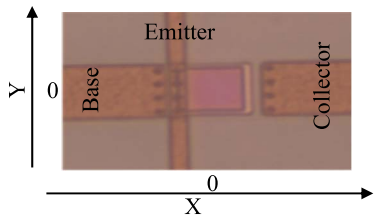

Fig. 14. The microscopic picture of the top view of the transistor.

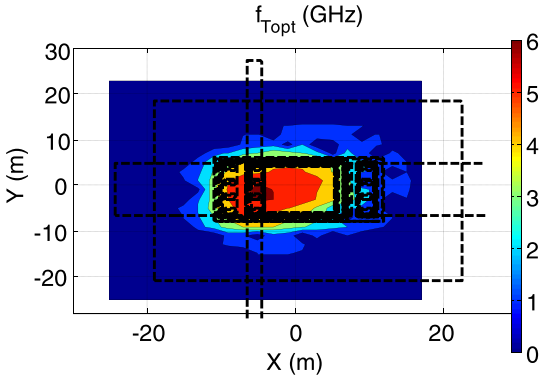

Fig. 15. The topological map of the optical transition frequency f_{Topt} at various locations of optical light illumination.

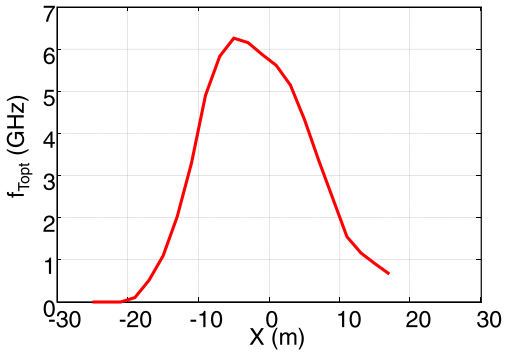

Fig. 16. The slice curve of the optical transition frequency f_{Topt} at Y=0μm.

(namely 52 GHz). This, obviously, demonstrates the impact of the photo-generated carriers on HPT frequency performance under opto-microwave operation. However, this maximal f_{Topt} value still indicates that this HPT could be implemented in optical applications operating up to 6.5 GHz.

We have also explicitly explored the influence of the HPT lateral structure on the frequency performance by performing opto-microwave Scanning Near-field Optical Microscopy (OM-SNOM) by translating the optical beam over the optical window surface. Figure 14 shows the microscopic picture of 10×10 μm^2 optical window size HPT over which the OM-SNOM is performed.

Figure 15 presents the intrinsic optical transition frequency versus the fiber position above the HPT along with the superimposed layout of the designed HPT.A slice curve of this cartography at Y=0 μm is shown in Figure 16. The f_{Topt} curve is symmetrical with respect to the Y axes; however it is not symmetric with respect to X axis as its peak appears

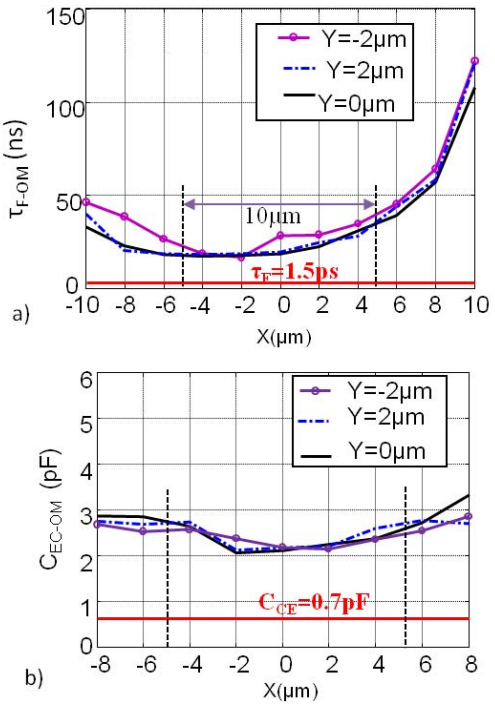

Fig. 17. The extracted opto-microwave a) forward transit time and b) emitter-collector junction capacitance at different optical injection positions over the phototransistor optical window. The electrical forward transit time (τ_F) and emitter-collector capacitance (C_{EC}) are plotted in figures a) and b) respectively.

close to the base and emitter. A maximum f_{Topt} of 6.2G Hz is measured at X=-5 μm and Y=0 μm. We recall the illumination position corresponding to f_{Topt} peak has been chosen for the measurement results given in Figure 13.

f_{Topt} peak is shifted from the center of the optical window towards the base and emitter contacts due to the 2 dimensional path for photo-generated holes to reach the base-emitter junction in the electrical extended active region where they will initiate the transistor effect. When the optical beam is injected close to the base and emitter contact, the distance travelled by the holes to reach the base and emitter contacts become very short, whereas when the optical beam is injected at the center of the optical window the distance travelled by the holes to reach the base and emitter contacts is longer as the related transit time.

To complete this analysis, we extracted the opto-microwave capacitances and transit times while displacing the optical fiber over HPT surface. Figure 17 a) and b) respectively show the slice curves of the opto-microwave transit time and junction capacitance at Y=0, -2 and 2 μm.

Important variations on the OM transit time (τ_{F-OM}) are observed over the HPT optical window. The highest value of τ_{F-OM} is obtained when the optical beam is close to the collector contact (at X=5μm), i.e. far from the emitter and base contacts. In this region the transit time is mainly controlled by the photo-generated holes traveling towards the base and emitter contacts. The minimum transit time value is obtain close to the base contact, i.e. far from the collector ones. In this area the transit time of the electrons to reach the collector contact is responsible for the measured OM transit time value.

The optimal transit time value is reached 2 μm to 4 μm away from the center of the optical window towards the base and emitter contacts. This opto-microwave transit time (τ_{F-OM}) is much higher than the electrical transit time ($\tau_F = 1.5$ps). This confirms that the photo-carriers generated in the active region under the optical window need longer time to reach the electrical contacts.

The opto-microwave junction capacitance does not vary a lot over the optical window as shown in Figure 17b). However, compared to the electrical junction capacitance ($C_{EC} = 0.7$ pF), it is increased by a factor of more than 3.

V. Scaling Limitations and Design Rules

The speed of a phototransistor could be improved through properly designing regarding the vertical thickness of its different layers. However, the main focus of this work is to use the existing HBT technology to fabricate the phototransistor or photodiode in order to minimize the total cost. As a result, the HPT fabrication process is adapted to the HBT technology by using the existing masks and following the industrial fabrication process without modifying the vertical layers and other properties of the technological process.

However, the designer can optimize the speed of the targeted HPT by properly designing its lateral dimensions and the optical window. As demonstrated above, both the length and width of the emitter highly influence the speed of the transistor due to the presence of the emitter peripheral current, the collector current spreading and the 2-D carrier flow. These effects have to be minimized through proper design of the structure.

To minimize the influence of the peripheral current and collector current spreading, the optimum HPT size has to be determined through a proper physical or electrical modeling of the structure that could be done using commercial software's.

Besides, the 2-D carrier flow effect can be minimized through proper design of the structure. Several solutions can be considered:

- Design a symmetrical collector, base and emitter contacts as it will lead to more vertical carrier flow.
- Fragmentation of the HPT into smaller individual HPTs, as the electrical extension region Δ may reach to the fragmented device size limit.
- Considering laterally illuminated structures [22], [23] to improve the HPT opto-microwave speed.

VI. Conclusion

The influence of lateral scaling on the important bipolar transistor characteristics such as transit time and junction capacitance is shown through intensive experimental results. The impact of emitter width and length are studied independently. During this study it is demonstrated that the HBT cutoff frequency, f_T decreases as the emitter length decreases from 20 μm to 3 μm for a given emitter width due to the predominance of the peripheral current for smaller size HBT.

For the opto-microwave applications, the phototransistor is fabricated by using the existing SiGe HBT technology without

modifying the vertical stacks and layers. Instead, the lateral dimensions of the active layer are increased by extending the emitter-base-collector layers with the emitter contact kept at its original position in order to create the optical access. We choose a square optical window in order to minimize the influence of the peripheral current. It is experimentally demonstrated that the optimum cutoff frequency f_T appears when the optical window is of 10×10 μm^2. The asymmetry between base and collector contacts generates the lateral flow of carriers which reduces the phototransistor speed. This effect is more predominant for HPTs of small optical window. For HPTs having optical window larger than 10×10 μm^2, the f_T decreases as the junction capacitances and resistances increase with the size.

We focused on 10×10 μm^2 optical window size HPT to show the dependency of the opto-microwave frequency behavior on the 2-D carrier flow effect. For that purpose, an OM SNOM analysis is performed over the surface of the HPT window in order to identify the fastest and the slowest regions. It is observed that the peak of the optical transition frequency appears close to the base-emitter. We observed that there is small variation of the OM junction capacitance value over the optical window. However, the transit time quickly increases as the optical beam moves towards the collector contact and its optimum smallest value appears towards the emitter-base contact.

To improve the frequency response, proper design rules are proposed that are to get symmetric collector, base and emitter contacts so that the electrical field is more vertical, to fragment the HPT into smaller individual HPTs as the electrical extension may reach a limit in its increase. Laterally illuminated HPT structure could also improve the opto-microwave speed.

REFERENCES

[1] C. Viana *et al.*, "Hybrid photo-receiver based on SiGe heterojunction photo-transistor for low-cost 60 GHz intermediate-frequency radio-over-fibre applications," *IEEE Electron. Lett.*, vol. 51, no. 8, pp. 640–642, Apr. 2015.

[2] J. Guillory, A. Pizzinat, B. Charbonnier, and C. Algani, "60 GHz intermediate frequency over fiber using a passive multipoint-to-multipoint architecture," in *Proc. IEEE NOC*, Newcastle-Upon-Tyne, U.K., Jul. 2011, pp. 44–47.

[3] Z. G. Tegegne *et al.*, "Substrate diode effect on the performance of silicon germanium phototransistors," in *Proc. IEEE MWP*, Paphos, Cyprus, Oct. 2015, pp. 1–4.

[4] J. L. Polleux, F. Moutier, A. L. Billabert, C. Rumelhard, E. Sonmez, and H. Schumacher, "A strained SiGe layer heterojunction bipolar phototransistor for short-range opto-microwave applications," in *Proc. IEEE- MWP*, Budapest, Hungary, Sep. 2003, pp. 113–116.

[5] J. L. Polleux, F. Moutier, A. L. Billabert, C. Rumelhard, E. Sönmez, and H. Schumacher, "An SiGe/Si heterojunction phototransistor for opto-microwave applications: Modeling and first experimental results," in *Proc. GAAS Conf. Eur. Microw. Week*, Munich, Germany, Oct. 2003, pp. 231–234.

[6] Z. Pei *et al.*, "Bandwidth enhancement in an integratable SiGe phototransistor by removal of excess carriers," *IEEE Electron Device Lett.*, vol. 25, no. 5, pp. 286–288, May 2004.

[7] M. Egels, B. Delacressonnière, Y. Sahabun, and P. Lecoy, "Design of an optically frequency or phase-controlled oscillator for hybrid fiber-radio LAN at 5.2 GHz," *Microw. Opt. Technol. Lett.*, vol. 45, no. 2, pp. 104–107, 2005.

[8] T. Yin, A. M. Pappu, and A. B. Apsel, "Low-cost, high-efficiency, and high-speed SiGe phototransistors in commercial BiCMOS," *IEEE Photon. Technol. Lett.*, vol. 18, no. 1, pp. 55–57, Jan. 1, 2006.

[9] K.-S. Lai, J.-C. Huang, and K. Y.-J. Hsu, "High-responsivity photodetector in standard SiGe BiCMOS technology," *IEEE Electron Device Lett.*, vol. 28, no. 9, pp. 800–802, Sep. 2007.

[10] J. Kim, S. Kanakaraju, W. B. Johnson, and C.-H. Lee, "InP/InGaAs uni-travelling carrier heterojunction phototransistors," *Electron. Lett.*, vol. 45, no. 12, pp. 649–651, Jun. 2009.

[11] A. Leven, V. Houtsma, R. Kopf, Y. Baeyens, and Y.-K. Chen, "InP-based double-heterostructure phototransistors with 135 GHz optical-gain cutoff frequency," *Electron. Lett.*, vol. 40, no. 13, pp. 833–834, Jun. 2004.

[12] M. D. Rosales, J.-L. Polleux, and C. Algani, "Design and implementation of SiGe HPTs using an 80 GHz SiGe bipolar process technology," in *Proc. GFP*, London, U.K., Sep. 2011, pp. 243–245.

[13] Z. G. Tegegne, "SiGe/Si microwave photonic phototransistors and interconnects towards silicon-based full optical links," Ph.D. dissertation, Univ. Paris-Est, Champs-sur-Marne, France, May 2016.

[14] J.-S. Rieh *et al.*, "SiGe heterojunction bipolar transistors and circuits toward terahertz communication applications," *IEEE Trans. Microw. Theory Techn.*, vol. 52, no. 10, pp. 2390–2408, Oct. 2004.

[15] M. Schroter and D. J. Walkey, "Physical modeling of lateral scaling in bipolar transistors," *IEEE J. Solid-State Circuits*, vol. 31, no. 10, pp. 1484–1492, Oct. 1996.

[16] G. Liu, A. Trasser, and H. Schumacher, "33–43 GHz and 66–86 GHz VCO with high output power in an 80 GHz f_T SiGe HBT technology," *IEEE Microw. Wireless Compon. Lett.*, vol. 20, no. 10, pp. 557–559, Oct. 2010.

[17] F. Moutier, J. L. Polleux, C. Rumelhard, and H. Schumacher, "Frequency response enhancement of a single strained layer SiGe phototransistor based on physical simulations," in *Proc. IEEE EGAAS*, Paris, France, Oct. 2005, pp. 113–116.

[18] M. Reisch, *High-Frequency Bipolar Transistors*. Springer, 2003.

[19] W. Hafez, J.-W. Lai, and M. Feng, "Vertical scaling of 0.25-μm emitter InP/InGaAs single heterojunction bipolar transistors with f_T of 452 GHz," *IEEE Electron Device Lett.*, vol. 24, no. 7, pp. 436–438, Jul. 2003.

[20] H.-M. Rein, "A simple method for separation of the internal and external (peripheral) currents of bipolar transistors," *Solid-State Electron.*, vol. 27, no. 7, pp. 625–631, 1984.

[21] D. J. Walkey, M. Schroter, and S. Voinigescu, "Predictive modelling of lateral scaling in bipolar transistors," in *Proc. Bipolar/Bicmos Circuits Technol. Meeting*, Oct. 1995, pp. 74–77.

[22] Z. G. Tegegne, C. Viana, J. L. Polleux, M. Grzeskowiak, and E. Richalot, "Edge illuminated SiGe Heterojunction Phototransistor for RoF applications," *Electron. Lett.*, vol. 51, no. 23, pp. 1906–1908, Nov. 2015.

[23] Z. G. Tegegne, C. Viana, J. L. Polleux, M. Grzeskowiak, and E. Richalot, "Improving the opto-microwave performance of SiGe/Si phototransistor through edge illuminated structure," in *Proc. SPIE, Photon. West Conf.*, vol. 9752. San Francisco, CA, USA, Feb. 2016, pp. 13–18.

Zerihun Gedeb Tegegne received the B.Sc. degree in electrical engineering from Arbamich University, Ethiopian, in 2007, the master's degree in optical communications and photonic technologies from the Politecnico di Torino, Italy, in 2012, and the Ph.D. degree in electronics, optoelectronics and systems from Université Paris-Est, France. He was a Post-Doctoral Researcher with the XLIM Research Institute, France. He is currently a Researcher with the ESYCOM Laboratory, ESIEE-Paris. His research interests include the study of integrated photonics, optoelectronic and microwave photonics multiplexing devices, radio-over-fiber systems, and microwave photonics radar imaging systems.

Carlos Viana was born in Viana do Castelo, Portugal, in 1986. He received the M.S. degree in electrical and computers engineering from the Faculty of Engineering, University of Porto, Porto, Portugal, in 2010, and the Ph.D. degree in electronics, optoelectronics and systems from Université Paris-Est, Champs-sur-Marne, France, in 2014. Since 2010, he has been a Researcher with the ESYCOM Laboratory, ESIEE-Paris, Noisy-le-Grand, France. His research interest includes optoelectronic device developments, integration, and packaging for low cost radio-over-fiber technology applications.

Jean-Luc Polleux received the master's/Diplôme d'ingénieur degree in microelectronic from ENSEIRB, Bordeaux, France, and the DEA degree in electronic and telecommunications from the University of Bordeaux 1, France, both in 1997, and the Ph.D. degree in the opto-microwave from CNAM, Paris, in 2001. He joined ESIEE-Paris, Université Paris-Est, France, and the joint ESYCOM Laboratory, where he is currently an Associate Professor. He is also an Administrator of Optics'Valley, Ile-de-France region, and the Head of the International Master of Electronics, ESIEE Paris, UPE. He published over 60 scientific publications and two patents. His current research involves microwave-photonics devices and systems for radio-over-fibre applications with special emphasis on microwave phototransistors (SiGe/Si and InGaAs/InP), silicon-based integration and packaging, analogue VCSELs, and opto-microwave devices modeling. He co-organized three international workshops and co-chaired the local committee of the French microwave conference JNM2013. He was a Guest Editor of the *International Journal of Microwave and Wireless Technologies* (IJMWT) in 2014.

Marjorie Grzeskowiak was born in France, in 1973. She received the M.Sc. and Ph.D. degrees in electronics and in microelectronics engineering from the Université des Sciences et Technologies de Lille, France, in 1996 and 1999, respectively. Her dissertation was on the design, simulation, realization, and measurement of the microwave antennas on GaAs substrate. In 2000, she joined the Electronic, Communication, Systems and Microsystems Laboratory, Université de Marne-la-Vallée, Marne-la-Vallée, France, as an Assistant Professor, where she is involved in the propagation and the design of the millimeter wave passive devices, and more recently in the study of the magnetic coupling. She is involved in the design, simulation, and measurement.

Elodie Richalot received the master's /Engineer Diploma degree in electronics engineering from ENSEEIHT, Toulouse, France, in 1995, and the Ph.D. degree in electronics engineering from INPT, Toulouse, in 1998. Since 1998, she has been with the University Paris-Est Marne-la-Vallée, Champs-sur-Marne, France, as an Associate Professor and then a Professor in electronics in 2010, where she is currently the Head of the Master of Electronics She is also the Head of the Research Group in electromagnetism at ESYCOM. Her current research interests include modeling techniques, electromagnetic compatibility, urban propagation, and millimeter wave transmission lines.